

# DESIGN AND PROCESSING CONDITIONS OF HYPOEUTECTIC Al-Cu-Sc ALLOYS FOR MAXIMUM BENEFIT OF SCANDIUM

A-A. Bogno<sup>1</sup>, H. Henein<sup>1</sup>, M. Gallerneault<sup>2</sup>

<sup>1</sup>Department of Chemical and Materials Engineering, University of Alberta  
Edmonton, Alberta, Canada T6G 1H9

<sup>2</sup>Alcereco Inc. Kingston, ON K7L3N6 Canada

Key words: Rapid solidification, atomization, Al-alloys, scandium, microstructures

## Abstract

Addition of Sc to Al-Cu is reported to be responsible for a high precipitation hardening upon heat treatment and serves as a good grain refiner. However, Scandium is presently very expensive, therefore, getting maximum benefit from a minimum addition would be economically of value. This work studies microstructures and mechanical properties of hypoeutectic Al-4.5wt%Cu-xSc ( $x = 0.1, 0.2$  or  $0.4$ wt %) of various thermal histories. Samples are generated under a wide range of cooling rates and undercooling by two different methods, including Differential Scanning Calorimetry and Impulse Atomization. In as-solidified as well as in heat treated conditions, the samples are investigated by means of Electron Microscopy, diffraction analysis and microhardness measurements. The results of this work identify those processing conditions that make optimum use of the Sc in enhancing the mechanical properties of the Al-Cu alloy.

## 1. Introduction

Aluminum (Al), one of the lightest engineering metal, has a high strength to weight ratio that makes it ideal for transport applications, where weight reduction and energy savings are environmentally valuable. When properly alloyed, Al represents the potential of a high strength material. In general, addition of Transition Metals (TM) such as Sc to aluminum results in the formation of finely dispersed precipitates upon heat treatment. Indeed, for all Al-TM systems the invariant transformation temperatures (eutectic and peritectic), are close to the melting point of Al and the Al-rich corner of these systems shows a very narrow solidification interval [1]. These characteristics, combined with the low diffusion coefficients of TM in liquid and solid aluminium, are the reasons for the tendency of Al-TM to form supersaturated solid solutions during solidification. Sc addition to Al-alloys suppresses recrystallization, strengthening and acts as a modifier [1].

Al-Cu, one of the most widely used base alloys also has a high age-hardening potential, characterized by the precipitation of finely dispersed Guinier-Preston (GP1 and GP2) zones,  $\theta'$ ,  $\theta''$  and ultimately the stable  $\theta$ -Al<sub>2</sub>Cu phase, generally upon heat treatment but also at room temperature [2,3]. Based on the potential of both Al-Cu and Al-Sc, a ternary Al-Cu-Sc would be technologically and industrially very interesting. However, it has been reported that the use of Sc in xxx Al-Cu alloys tends to form detrimental ternary AlCuSc particles (W-phase) [4-8] that consume most of the Cu and Sc atoms that are available for the formation of supersaturated solid solution, resulting in the decrease of precipitation of the strengthening Al<sub>2</sub>Cu, Al<sub>3</sub>Sc phases upon aging treatment which consequently results in the decrease of the material strength [9,10].

This present paper investigates hypo-eutectic Al-4.5wt% Cu with different Sc levels (0.1, 0.2 and 0.4wt %) solidified relatively slowly by Differential Scanning Calorimetry (DSC) and rapidly by Impulse Atomization (IA). Different heat treatments of the as solidified samples are then carried out. The aim of this work is to find such processing conditions that make optimum use of the Sc by minimizing or completely avoiding the formation of the detrimental W phase so that the mechanical properties of the Al-Cu alloy are improved.

## 2. Formation of the W- phase

The W- phase crystallises in a tetragonal structure of the ThMn<sub>12</sub>-type, with unit-cell parameters of  $a = 0.863$  nm and  $c = 0.510$  nm [11]. Its chemical composition is Al<sub>8+x</sub>Cu<sub>4+x</sub>Sc ( $0 < x < 2.6$ ), which forms over a limited compositional range and also has the same structure as ScFe<sub>4</sub>Al<sub>8</sub> [12,13]. The formation of W- phase may happen following two pathways, both related to the  $\theta$ -Al<sub>2</sub>Cu intermetallic [14]. The first pathway includes its growth on an existing Al<sub>2</sub>Cu phase and the second is a resulting product of the transformation of the Al<sub>2</sub>Cu phase inherent to the diffusion of Sc from the Al solid solution (Figure 1).

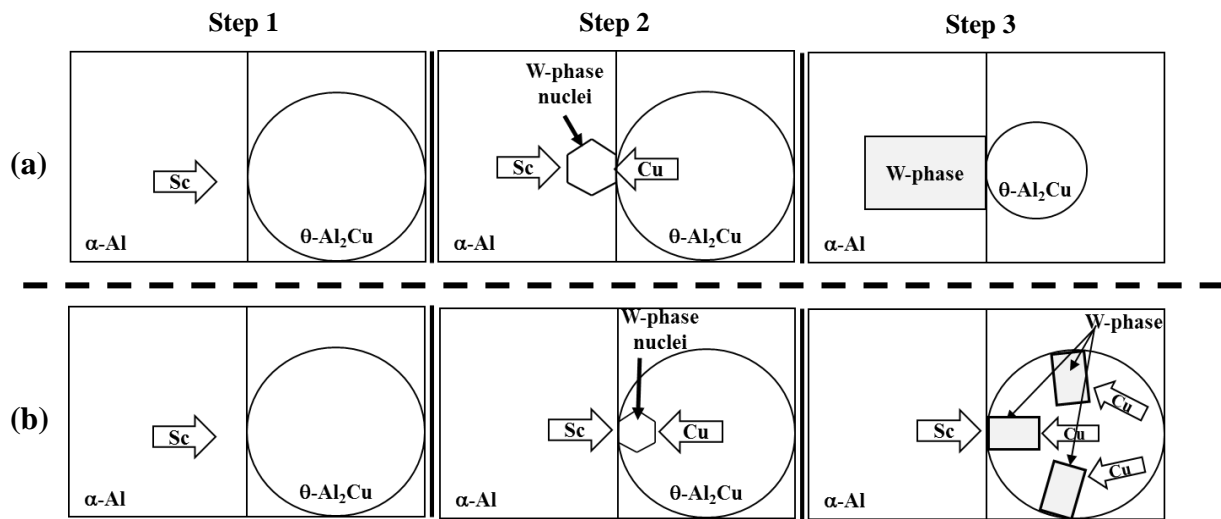


Figure 1: The two pathways for the formation of the W-phase described in 3 steps: (a) nucleation on the  $\theta$ -Al<sub>2</sub>Cu phase (b) transformation from  $\theta$ -Al<sub>2</sub>Cu phase inherent to the diffusion of Sc from the Al solid solution [14].

Thus,  $\theta$ -Al<sub>2</sub>Cu phase, formed during solidification, appears to be the precursor of the W-phase formation. The formation of W-phase following these two pathways is likely to occur during homogenization when sufficient time is allowed for the Sc and Cu atoms to diffuse through the matrix so that Al<sub>2</sub>Cu is transformed into W-phase. This has been demonstrated by the solution heat treatment of 1469 alloy in melted salt bath at 515°C for 1h and then quenched into water [15,16] or by the homogenization of a Sc-containing Al-Cu-Mg-Ag alloys at 510°C for 24h [14].

In addition to the above mentioned two pathways for the formation of W-phase, Figure 2 shows a prediction by Gulliver-Scheil solidification (of an Al-4.5wt% Cu-0.4 wt% Sc) obtained by ThermoCalc, using TCAL4 database [17]. The simulation suggests that the W-phase also takes part in two invariant reactions, including, Liquid  $\rightarrow$  W +  $\alpha$ -Al +  $\theta$ -Al<sub>2</sub>Cu at 546°C and the peritectic reaction: Liquid + Al<sub>3</sub>Sc  $\rightarrow$   $\alpha$ -Al + W at 572°C. The database TCAL4 used for this prediction is based on the work done by Kharakterova [8]. These results are also reported in [7,8], [10,18,19]. A thermodynamic assessment of the Al-Cu-Sc system in the Al-rich corner by Bo et al [6] confirms the two invariant reactions. However, they mentioned that there was a discrepancy between the calculations and the experimental data regarding the maximum solubility for Al in the  $\alpha$ -Al + W + Al<sub>3</sub>Sc three-phase equilibrium. The calculated result yields about 2.4 wt. % Cu, whereas the reported experimental data is 0.56 wt. % Cu.

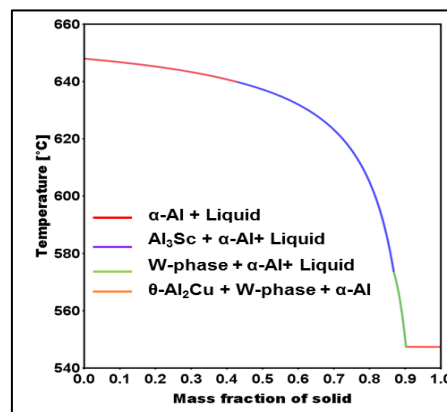


Figure 2: Gulliver-Scheil prediction of phase formation during solidification of Al-4.5 wt% Cu-0.4 wt% Sc alloy, obtained through the TCAL4 database of Thermo-Calc [20].

### 3. Slow solidification processing

#### 3.1. Samples production

Slowly solidified Al-4.5wt%Cu-xSc ( $x = 0.1, 0.2$  or  $0.4$ wt %) samples were produced by a Setaram Labsys Evo 1600 differential scanning calorimeter (DSC) using two alumina crucibles (sample and reference crucibles) and a platinum-rhodium sensor. The calorimeter was calibrated for a wide range of temperatures and heat measurements using standard samples of Al, Ag, Zn, Sn, and Au. For the present investigation, the samples were heated by an S-type thermocouple (Pt / Pt Rh 10%) regulated furnace under a continuously sweeping argon atmosphere. A scanning rate of  $2^{\circ}\text{C}/\text{min}$  was applied to bring the sample temperature to  $850^{\circ}\text{C}$  before cooling. For this investigation, different cooling rates were applied, varying from  $0.5^{\circ}\text{C}/\text{min}$  up to  $50^{\circ}\text{C}/\text{min}$ . The temperature variation of the samples was recorded by means of a thermocouple placed between the two alumina crucibles.

#### 3.2. Analysis techniques

The solidification microstructures were examined using different but complementary analytical tools. After solidification by DSC, the samples were ground and polished in order to reveal the scale of microstructures. The examination of the microstructures was achieved by optical microscopy (using a motorized BX61 Olympus optical microscope) and Scanning Electron Microscopy (SEM) using a VEGA3 TESCAN instrument equipped with an EDX analysis system (INCA Microanalysis System, Oxford Instruments).

The scale of the microstructure was determined by the measurement of cell spacing, defined by the dendrite cell intervals (center-to-center distance between two dendrite cells). The cell intervals are approximated with the size of the cells so that using line intercepts method accordingly with ASTM E112-13, measurements of cell intervals were performed on the micrographs obtained by SEM (in back scattered electron (BSE) mode).

Hardness of as-solidified as well as heat treated samples were measured by a Buhler VH 3100 microhardness machine. The device was calibrated using a manufacturer provided steel block. Five indentations were randomly applied on each sample with a load of 100gf held for 10s.

#### 3.3. Results

Microstructural analysis of the Al-4.5 wt% Cu with different Sc additions (0.1 wt%, 0.2 wt% and 0.4 wt %) solidified at different cooling rates, varying from  $0.1^{\circ}\text{C}/\text{s}$  to  $0.8^{\circ}\text{C}/\text{min}$  was carried out. As can be seen in Fig.1, the addition of Sc does not refine the microstructures within the investigated cooling rates; instead Sc modifies the grain morphologies from elongated dendrites to more equiaxed grains.

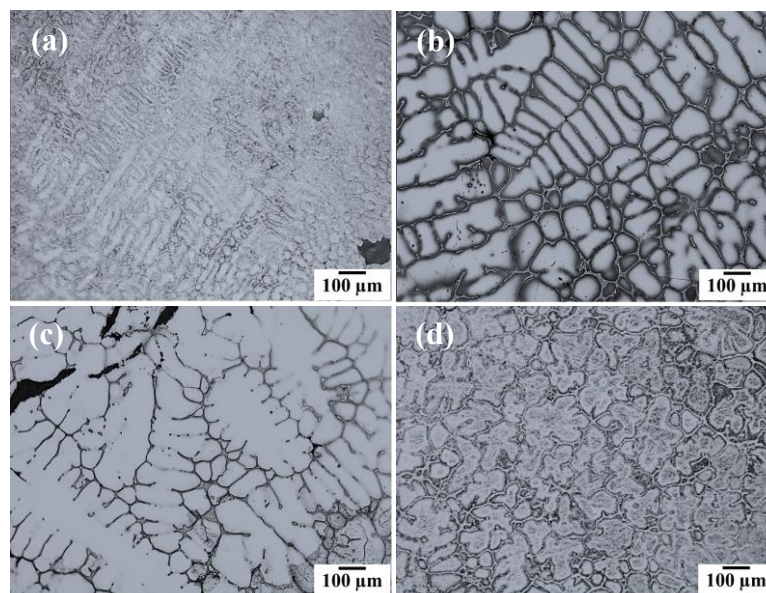


Fig.3: Optical micrographs of representative solidification microstructures of investigated Al-4.5 wt% Cu alloys with different Sc additions cooled at the  $0.8^{\circ}\text{C}/\text{s}$ ; (a) 0.0 wt% Sc, (b) 0.1 wt% Sc, (c) 0.2 wt% Sc and (d) 0.4 wt% Sc.

Mechanical properties were evaluated via Vickers microhardness measurements on as-solidified as well on heat treated samples. A typical industrial heat treatment procedure for Al-alloys was applied. It consisted on solutionizing at 535°C for 18.5 h (for homogenization) and quenching with dry ice, followed by aging at 240°C for 2h.

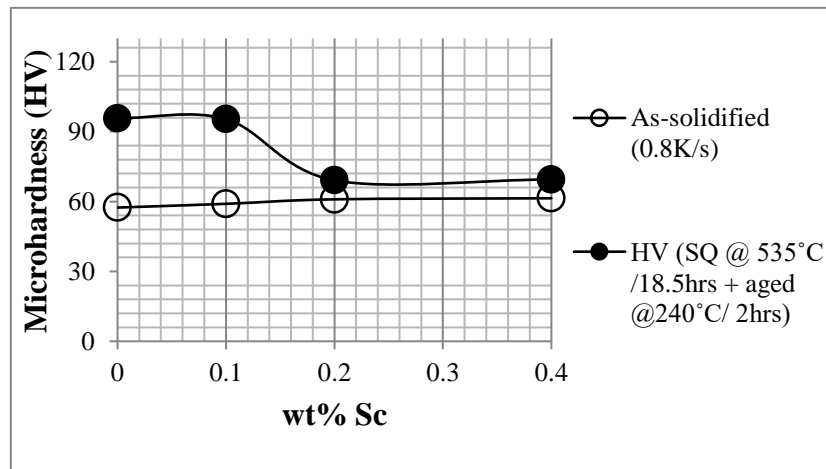


Fig. 4: Variation in Vickers microhardness with Sc concentration in Al-4.5 wt% Cu (Sc) alloys after solutionizing at 535°C for 18.5 hours and quenching in a beaker filled with crushed dry ice before aging at 240°C for 2 hours.

Fig.4 shows the microhardness (VH) variation as a function of Sc for both as-solidified and heat treated samples. As can be seen, the variation with Sc content is negligible in as-solidified conditions, suggesting that the addition of Sc to the hypoeutectic Al-Cu alloy is not an effective strengthener under low solidification rate processing conditions. After heat treatment, Fig.4 shows an increased microhardness for all Sc levels. However, it is worth noting that samples with Sc level < 0.1wt% show higher hardness, suggesting that more precipitation of strengthening phases [16] (mainly Al<sub>2</sub>Cu at this level of Sc) occurred after aging, subsequent to homogenization and quenching.

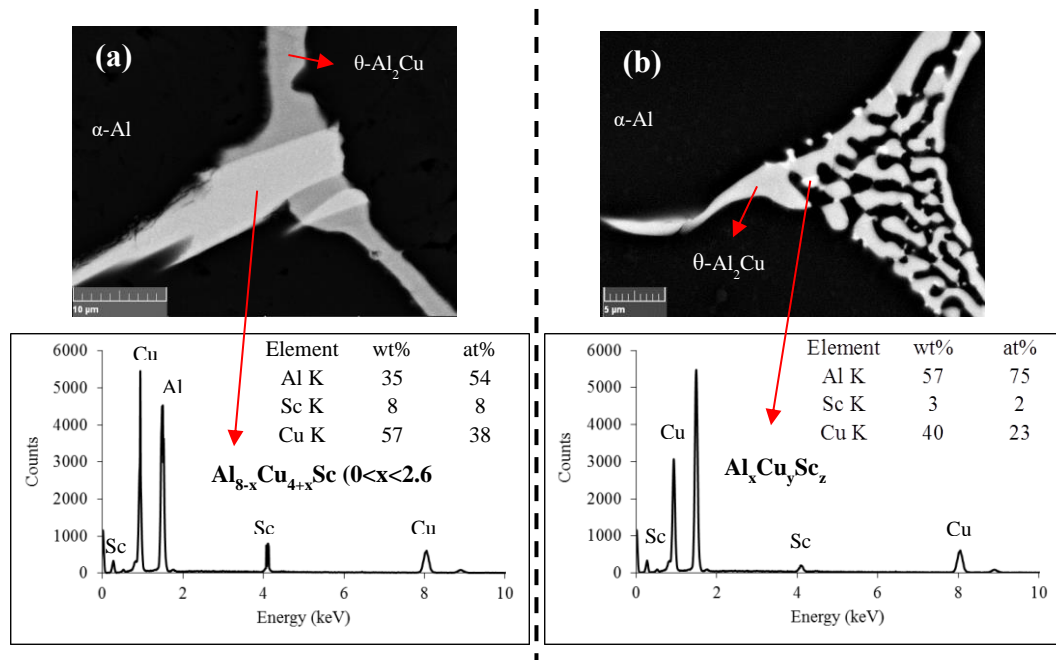


Fig.5: Microstructure analysis for Al-4.5 wt% Cu-0.4 wt% Sc alloy: (a) SEM BSE image of primary  $\alpha$ -Al phase and the eutectic structure for a cooling rate of 0.1°C/s. (b) EDX spectrum from the Al-Cu-Sc ternary phase precipitate. (c) SEM BSE image of primary  $\alpha$ -Al phase and intermetallic for a cooling rate of 0.8°C/s. (d) EDX spectrum from intermetallic phase in the inter-dendritic region.

For samples with higher levels of Sc ( $> 0.1$  wt %), the lower hardness values may be due to the incomplete / non-dissolution of Sc- and Cu-rich W-phase, observed in the as-solidified microstructures (Fig.5). Indeed, as shown by EDX spectra in Fig.5a and Fig.5b, the W- phase consumes a large amount of Cu atoms and some amount of Sc, consequently, the amount of supersaturated Cu and Sc atoms in the  $\alpha$ -Al phase is reduced, thereby, reducing the volume fraction of  $\text{Al}_2\text{Cu}$  and  $\text{Al}_3\text{Sc}$  hardening phases. It is worth noting that the size of the W-phase precipitates decreases with increasing cooling rate, so that under rapid solidification conditions, a complete disappearance of W-phase may result.

#### 4. Rapid solidification processing

##### 4.1. Samples production

Rapid solidified samples were generated by Impulse Atomization (IA) under Ar and He. A detail description of the technique is given elsewhere [22, 23]. For this investigation, 350g of each alloy composition were melted by induction in a graphite crucible. The temperature was brought up to  $850^\circ\text{C}$  ( $\sim 200^\circ\text{C}$  above the liquidus temperature) before atomization in an almost oxygen free (10ppm) chamber. Atomized powders of different sizes (different thermal histories) varying from  $>212\ \mu\text{m}$  to  $1000\ \mu\text{m}$  were obtained. Nucleation temperature and cooling rate of the falling droplets during atomization could not be measured, however, thermal history of each droplet is predicted using a numerical model developed by Wiskel et al [23,24] and nucleation undercooling was determined using a method that we developed and published in [25].

##### 4.2. Analysis and Results

Characterization of the samples generated by IA was carried out using the same analytical tools used to analyze the slow solidified samples by DSC. In addition, the microstructural phases were identified using a Rigaku Geigerflex Powder Diffractometer. The diffractions were recorded within a wide range of angles ( $2\theta$ ) varying from  $5^\circ$  to  $90^\circ$  with a step of  $0.02^\circ$  and a holding time of 0.60s at each step. During the analysis, the X-ray tube had a 38mA current under 38KV. A  $\text{CoK}\alpha_1$  radiation with a wavelength of  $1.78899\text{\AA}$  to calculate d-spacing. Fig.6 shows diffraction patterns of the investigated Al-4.5wt Cu-xSc ( $x=0.1, 0.2,$  and  $0.4$ wt %) powders. It appears that the microstructures of the as-atomized samples consist of  $\alpha$ -Al and  $\theta$ - $\text{Al}_2\text{Cu}$ , without any Sc-rich phase being detected.

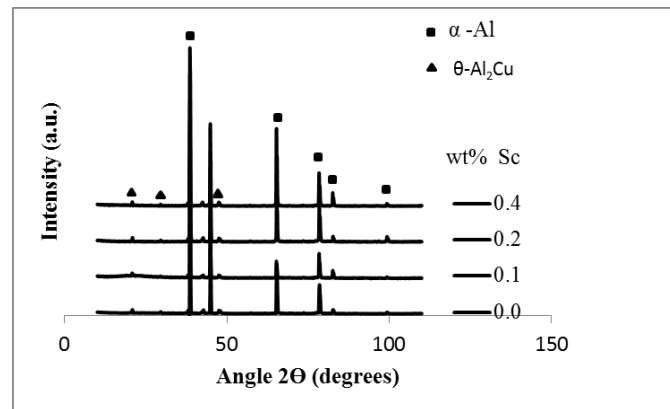


Fig.6. X-ray diffraction diagrams of IA Al-4.5wt% Cu - x Sc powders

Fig.7 shows a representative micrograph of the powders investigated in this work. As evidenced by the surface grain structure, the microstructures are of cellular morphologies, suggesting that the atomized droplets experienced rapid solidification, characterized by a high growth velocity (Fig. 6b) as described by Kurz & Fisher [26]. It is worth noting that the analysis of the powders cross section by SEM showed no evidence of Sc-rich phase precipitations.

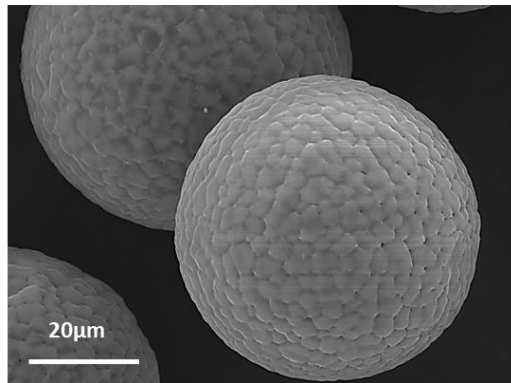


Fig.7 (a) SEM micrographs (BSE mode) of a representative investigated powder with visible surface grain structure. Alloy composition: Al-4.5 wt% Cu -0.4wt%Sc, atomization atmosphere: He; size range < 212 μm

Fig.8 shows the variation of cell spacing with cooling rate for different Sc levels. The rapid solidified microstructures are so fine that the effect of Sc is negligible.

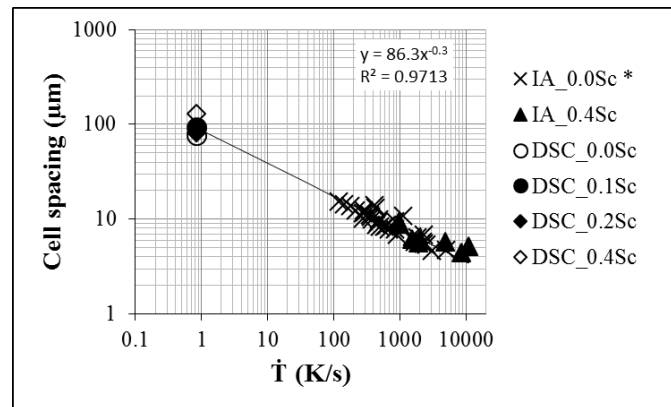


Fig.8: Variation of cell spacing with cooling rate for Al-4.5 wt% Cu with up to 0.4 wt% Sc of different thermal histories. (\*) represent published data by Wiskel et al. [24].

Cell spacing variation with solidification cooling rate is described by an equation of the form  $\lambda_2 = A\dot{T}^{-n}$ , where  $\lambda_2$  represents the cell spacing (in  $\mu\text{m}$ ), the solidification cooling rate (in  $^{\circ}\text{C}\text{s}^{-1}$ ) and A and n are alloy-dependent parameters, A being described as a “composition sensitive” by Eskin et al [27]. In this investigation, the values of A and n are in the range of values published by Mullis et al in [28] for powders produced by gas atomization.

Mechanical properties of the as-atomized as well as heat treated samples were evaluated through Vickers microhardness measurements. Two approaches were used for heat treatment of the as-atomized samples. The first approach is similar to the one applied for the DSC samples and the second heat treatment consisted in directly aging the as-atomized samples at 300°C for 20 hours, as the matrix is supposed to be supersaturated due to high undercooling induced rapid solidification [25, 29].

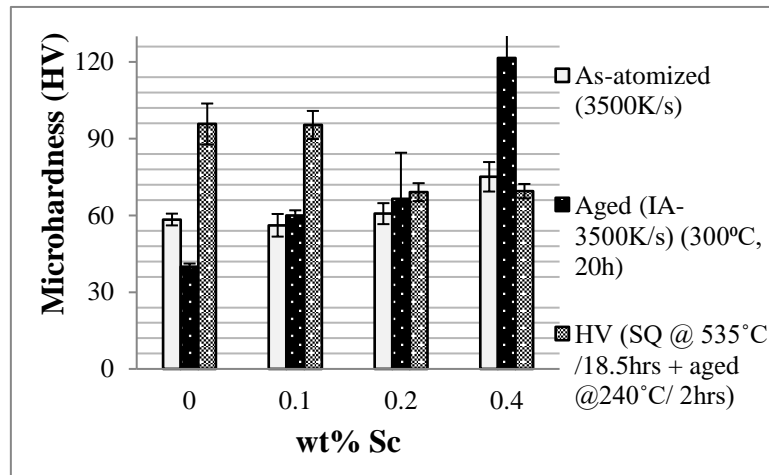


Fig.9: Variation of Vickers microhardness with Sc level in Al-4.5 wt% Cu (Sc) powders of different thermal histories:

Fig.9 shows the variation of hardness with Sc level in Al-4.5wt% Cu powders of different thermal histories, including as-atomized, aged after atomization and solutionized-quenched-and-aged. It is shown that microhardness increases slightly with Sc in the as-atomized samples. Indeed, the more the Sc in the initial liquid, the more supersaturated will the primary  $\alpha$ -Al be upon rapid solidification and consequently the harder will the as-atomized sample be. After solutionizing at 535°C for 18.5h and quenching, followed by aging at 240°C for 2h, the microhardness variation with Sc content, shows the same behaviour as for the DSC samples that went through the same heat treatment. It was concluded for the DSC samples that the decrease of hardness at Sc level > 0.1wt% was due to the reduction of volume fraction of strengthening  $Al_2Cu$  and  $Al_3Sc$  phases due to the non-dissolution of Cu- and Sc-consuming W-phase that had formed under slow solidification conditions. In the case of these atomized powders, XRD and SEM results showed that there is no formation of W-phase. Therefore, W-phase must have formed during homogenization following one of the pathways described in section 2. Indeed, An SEM image of the microstructures was taken after solutionizing and quenching (Fig.10). As can be seen in Fig.10a, there still remain some precipitates along the grain boundaries after solutionizing Al-4.5wt%Cu-0.4wt%Sc, while, a micrograph of an Al-4.5wt% Cu powder shows evidence of a complete dissolution of intermetallics after solutionizing under the same conditions (Fig.10b).

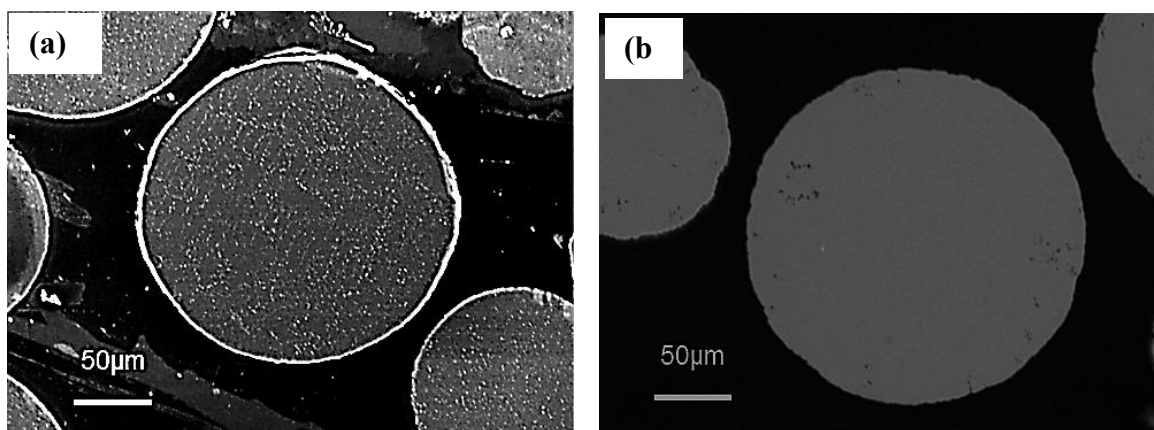


Fig.10: SEM (BSE) images of Al-4.5wt% Cu droplet solutionized at 535°C for 18.5h and quenched in dry ice (a) Sc level of 0.4wt%. Average size 230µm; Cooling gas He; (b) no Sc addition.

To identify the precipitates observed in Fig10a, a selective matrix dissolution was carried out on the solutionized and quenched samples. The process consisted in immersing the samples in an aqueous solution consisting of 40 g/l tartaric acid and 10 g/l  $FeCl_3$  for 4 hours in an ultrasound bath, as proposed by Michalcová et al for the matrix dissolution of a rapid solidified Al-Fe-Cr-Ti-Ce alloy [30]. Although the dissolution was not complete in this case for Al-Cu-Sc, the fraction of  $\alpha$ -Al phase was greatly reduced so that XRD examination of the resulting particles shows evidence of W-phase peaks (Fig.11), which otherwise would be too small to be visible peaks. In addition

to the  $\alpha$ -Al and W-phase, Cu peaks resulting from the diffraction of Cu that was dissolved in the matrix, were observed in Fig.11, proof of a selective dissolution of Al in the matrix [30].

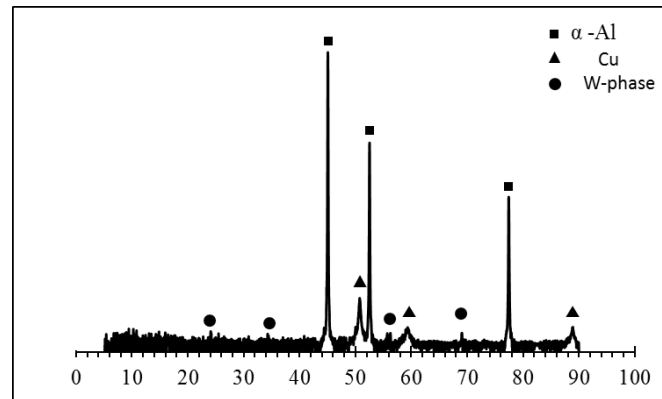


Fig.11. X-ray diffraction diagrams of extracted phases from solutionized and quenched ( $535^{\circ}\text{C}$  for 18.5h) Al-4.5wt% Cu-0.4wt% Sc droplets (size range  $212\text{-}250\mu\text{m}$ ), after a selective aluminium dissolution in an aqueous solution of 40g/l tartaric acid and 10 g/l  $\text{FeCl}_3$ .

For samples directly aged at  $300^{\circ}\text{C}$  for 20h after atomization, Fig.9 shows that the microhardness gradually increases with Sc content. At the highest level of Sc (0.4wt %) the value reaches 120Hv, which is much higher than the microhardness of all the investigated samples. This value, converted to yield stress, is about 250 MPa [31]. This increase in microhardness may be due to the precipitations of the strengthening  $\text{Al}_2\text{Cu}$  and  $\text{Al}_3\text{Sc}$  phases during the aging process. The identification of these precipitates is beyond the scope of this paper. This result suggests that by aging a rapidly solidified hypoeutectic Al-Cu-Sc, not only the heat treatment processing steps are shortened but also superior mechanical properties are obtained. Higher resolution imaging are required to identify the age hardening precipitates.

## 5. Conclusions

Al-4.5 wt% Cu alloys with different Sc content (0.1 wt%, 0.2 wt% and 0.4 wt %) were slow solidified by DSC and rapid solidified by IA. Samples with different thermal histories were generated by varying the cooling rate from  $0.1^{\circ}\text{C/s}$  to  $0.8^{\circ}\text{C/min}$  in the DSC and powders of sizes varying from  $>212\mu\text{m}$  to  $1000\mu\text{m}$  were produced by IA. The effects of cooling rate and Sc level on the microstructures scale, phase formation and mechanical properties were analysed.

While Sc modifies the solidification microstructures from elongated dendrites to equiaxed structure, its effect is found to be determined by the solidification rate.

Under low solidification rate conditions, the addition of Sc to hypo-eutectic Al-Cu alloys is not effective as an age hardener. Much of the Sc and Cu atoms are consumed in the formation of the intermetallic W-phase which remains undissolved after solutionizing. Consequently, applying a typical industrial heat treatment procedure yields no hardening effect because of the reduction of volume fraction of the strengthening  $\text{Al}_2\text{Cu}$  and  $\text{Al}_3\text{Sc}$  precipitates caused by the formation of W-phase. The size of the W-phase is found to be decreasing with increasing cooling rate so that it is completely avoided by rapid solidification processing as Sc supersaturates in the  $\alpha$ -Al matrix. The mechanical properties are found to increase considerably after aging the rapid solidified samples. Therefore, direct aging of a rapid solidified hypoeutectic Al-Cu-Sc is the better processing route as it is time and cost effective as it would eliminate solutionizing and quenching operations.

## Acknowledgements

The authors are grateful to the Natural Sciences and Engineering Research Council (NSERC) of Canada for their financial support. Thanks are also due to Novelis for providing the raw materials and Paul Mason for his help in providing the ThermoCalc database used in this paper.



## References

- [1] V. Davydov, T. Rostova, V. Zakharov, Y. Filatov, and V. Yelagin, "Scientific principles of making an alloying addition of scandium to aluminium alloys," *Mater. Sci. Eng. A*, vol. 280, no. 1, pp. 30–36, 2000.
- [2] M. J. Starink, N. Gao, and J. L. Yan, "The origins of room temperature hardening of Al-Cu-Mg alloys," *Mater. Sci. Eng. A*, vol. 387–389, no. 1–2 SPEC. ISS., pp. 222–226, 2004.
- [3] A. Cochard *et al.*, "Natural aging on Al-Cu-Mg structural hardening alloys – Investigation of two historical duralumins for aeronautics," *Mater. Sci. Eng. A*, vol. 690, pp. 259–269, 2017.
- [4] J. Røyset and N. Ryum, "Scandium in aluminium alloys," *Int. Mater. Rev.*, vol. 50, no. 1, pp. 19–44, 2005.
- [5] A. Norman, P. Prangnell, and R. McEwen, "The solidification behaviour of dilute aluminium-scandium alloys," *Acta Mater.*, vol. 46, no. 16, pp. 5715–5732, 1998.
- [6] H. Bo, L. B. Liu, and Z. P. Jin, "Thermodynamic analysis of Al-Sc, Cu-Sc and Al-Cu-Sc system," *J. Alloys Compd.*, vol. 490, no. 1, pp. 318–325, 2010.
- [7] L.S.Toropova, D.G.Eskin, M.L.Kharakterova, T.V.Dobatkina, *Advances in Aluminum Alloys Containing Scandium*. Amsterdam: Gordon and Breach Science publishers, 1998.
- [8] M. L. Kharakterova, "Phase composition of Al-Cu-Sc alloys at temperatures at 450 and 500 Deg.C," *Izv. Akad. Nauk SSSR, Met.*, vol. 4, pp. 191–194, 1991.
- [9] M. L. Kharakterova, D. G. Eskin, and L. S. Toropova, "Precipitation hardening in ternary alloys of the Al-Sc-Cu and Al-Sc-Si systems," *Acta Metall. Mater.*, vol. 42, no. 7, pp. 2285–2290, Jul. 1994.
- [10] D. Emadi, A. K. P. Rao, and M. Mahfoud, "Influence of scandium on the microstructure and mechanical properties of A319 alloy," *Mater. Sci. Eng. A*, vol. 527, no. 23, pp. 6123–6132, 2010.
- [11] W. Suski, T. Cichorek, K. Wochowski, D. Badurski, B. Y. Kotur, and O. I. Bodak, "Low-temperature electrical resistance of the U(Cu, Ni)<sub>4</sub>Al<sub>8</sub> system and magnetic and electrical properties of ScCu<sub>4+x</sub>Al<sub>8-x</sub>," *Phys. B Condens. Matter*, vol. 230–232, 1997.
- [12] H. Misiorek, J. Stępień-Damm, W. Suski, E. Talik, B. Kotur, and V. Dmitriev, "Lattice parameters, magnetic susceptibility and thermal conductivity of ScFe<sub>4</sub>Al<sub>8</sub> and YFe<sub>4</sub>Al<sub>8</sub>," *J. Alloys Compd.*, vol. 363, no. 1, pp. 81–87, 2004.
- [13] B. Y. Kotur, D. Badurski, W. Suski, K. Wochowski, A. Gilewski, and T. Mydlarz, "Structure, magnetic and electrical properties of ScFe<sub>x</sub>Al<sub>12-x</sub> alloys and their relation to the UFe<sub>x</sub>Al<sub>12-x</sub> system," *Phys. B Condens. Matter*, vol. 254, no. 1–2, pp. 107–111, Nov. 1998.
- [14] M. Gazizov, V. Teleshov, V. Zakharov, and R. Kaibyshev, "Solidification behaviour and the effects of homogenisation on the structure of an Al-Cu-Mg-Ag-Sc alloy," *J. Alloys Compd.*, vol. 509, no. 39, pp. 9497–9507, 2011.
- [15] M. Jia, Z. Q. Zheng, and X. F. Luo, "Influence of AlCuSc Ternary Phase on the Microstructure and Properties of 1469 Alloy," *Mater. Sci. Forum*, vol. 794–796, pp. 1057–1062, 2014.
- [16] M. Jia, Z. Zheng, and Z. Gong, "Microstructure evolution of the 1469 Al-Cu-Li-Sc alloy during homogenization," *J. Alloys Compd.*, vol. 614, pp. 131–139, 2014.
- [17] J. O. Andersson, T. Helander, L. Höglund, P. Shi, and B. Sundman, "Thermo-Calc & DICTRA, computational tools for materials science," *Calphad Comput. Coupling Phase Diagrams Thermochem.*, vol. 26, no. 2, pp. 273–312, 2002.
- [18] J. Royset, "Scandium in Aluminium alloys overview: Physical Metallurgy, Properties and applications," *Metall. Sci. and Technology*, vol. 25, no. 2, pp. 11–21, 2007.
- [19] A. Norman, P. Prangnell, and R. McEwen, "The solidification behaviour of dilute aluminium-

- scandium alloys,” *Acta Mater.*, vol. 46, no. 16, pp. 5715–5732, 1998.
- [20] “Thermo-Calc Database, TCAL4.” 2008.
- [21] H. Henein, “Single fluid atomization through the application of impulses to a melt,” *Mater. Sci. Eng. A*, vol. 326, no. 1, pp. 92–100, 2002.
- [22] H. Henein, V. Uhlenwinkel, and U. Fritsching, *Metal Sprays and Spray Deposition*. Springer, 2017.
- [23] J. B. Wiskel, H. Henein, and E. Maire, “Solidification study of aluminum alloys using impulse atomization: Part I - Heat transfer analysis of an atomized droplet,” *Can. Metall. Q.*, vol. 41, no. 1, pp. 97–110, 2002.
- [24] J. B. Wiskel, K. Navel, H. Henein, and E. Maire, “Solidification study of aluminum alloys using Impulse Atomization: Part II. Effect of cooling rate on microstructure,” in *Canadian Metallurgical Quarterly*, vol. 41, no. 2, pp. 193–204, 2002.
- [25] A.-A. Bogno, P. D. Khatibi, H. Henein, and C.-A. Gandin, “Quantification of Primary Dendritic and Secondary Eutectic Nucleation Undercoolings in Rapidly Solidified Hypo-Eutectic Al-Cu Droplets,” *Metall. Mater. Trans. A* vol. 47,no.9, pp. 4606-4615, 2016.
- [26] W.Kurz and D.J.Fisher, *Fundamentals of Solidification*, 4th editio. CRC Press, 1998.
- [27] D. Eskin, Q. Du, D. Ruvalcaba, and L. Katgerman, “Experimental study of structure formation in binary Al-Cu alloys at different cooling rates,” *Mater. Sci. Eng. A*, vol. 405, no. 1–2, pp. 1–10, 2005.
- [28] A. M. Mullis, L. Farrell, R. F. Cochrane, and N. J. Adkins, “Estimation of cooling rates during close-coupled gas atomization using secondary dendrite arm spacing measurement,” *Metall. Mater. Trans. B Process Metall. Mater. Process. Sci.*, vol. 44, no. 4, pp. 992–999, 2013.
- [29] J. H. Perepezko, J. L. Sebright, P. G. Hockel, and G. Wilde, “Undercooling and solidification of atomized liquid droplets,” *Mater. Sci. Eng. A*, vol. 326, pp. 144–153, 2002.
- [30] A. Michalcová, D. Vojtěch, and P. Novák, “Selective aluminum dissolution as a means to observe the microstructure of nanocrystalline intermetallic phases from Al-Fe-Cr-Ti-Ce rapidly solidified alloy,” *Micron*, vol. 45, pp. 55–58, 2013.
- [31] E. J. Pavlina and C. J. Van Tyne, “Correlation of Yield strength and Tensile strength with hardness for steels,” *J. Mater. Eng. Perform.*, vol. 17, no. 6, pp. 888–893, 2008.